ELSEVIER

Polymer 42 (2001) 3153–3160

polymer

www.elsevier.nl/locate/polymer

Properties of polyketone/polypropylene blends

E. Marklund[a], U.W. Gedde[a], M.S. Hedenqvist[a,*], G. Wiberg[b,1]

[a]*Department of Polymer Technology, Royal Institute of Technology, SE-100 44 Stockholm, Sweden*
[b]*Electrolux Research and Innovation AB, S:t Göransgatan 143, SE-105 45 Stockholm, Sweden*

Received 9 May 2000; received in revised form 12 July 2000; accepted 11 August 2000

Abstract

Blends of polypropylene and two polyketone grades with low and medium-high viscosities were prepared by melt extrusion. To obtain good compatibility, a maleic-anhydride–polypropylene copolymer was added to the blends. Polyoxypropylenediamine was added to some of the blends to further enhance compatibility. The blends were analysed with differential scanning calorimetry. In a second step, the blends were compression or injection moulded. Scanning electron microscopy, shear viscosity, density measurements and infrared spectroscopy were used to characterise the moulded blends and their oxygen permeabilities were assessed. Impact strength and hardness were measured on injection-moulded blends. It was shown that the oxygen barrier properties of polypropylene could be greatly enhanced by a small addition of primarily the low-viscosity polyketone. A content of 23.9% by volume of polyketone was sufficient to lower the permeability by 70% compared to pure polypropylene. This was because a polyketone-rich surface layer was formed during compression moulding. The incorporation of polyoxypropylenediamine had a profound effect on the morphology. The polyketone particles in this case were very small, and the absence of "pull-outs" suggested an enhanced phase adhesion between the different components. Further, the incorporation of polyoxypropylenediamine had no impact on the oxygen permeability but the impact toughness and hardness were increased and the shear viscosity was also increased in its presence. This indicated that chemical bonds were formed between polyketone, polyoxypropylenediamine and the maleic-anhydride–polypropylene copolymer. This network suppressed crystallisation of primarily the polyketone component.

Keywords: Polyketone; Blends; Oxygen permeability

1. Introduction

Random or alternating ethylene–carbon monoxide copolymers or ethylene–propylene–carbon monoxide terpolymers ('polyketones'), have lower gas permeabilities than polyethylene or polypropylene [1,2]. In addition they are less sensitive to chemicals and water than ethylene–vinyl copolymers, and this makes them suitable as replacements for the latter polymer in food packaging applications [2,3]. The latest generation of polyketones also possess high toughness and high temperature stability [2], whereas the first generation of highly alternating ethylene–carbon monoxide polymers were stiff and brittle due to their high crystallinity [4–6]. The latest generation of polyketones was obtained by adding a small amount of propylene during polymerisation [2]. The resulting terpolymer has a lower crystallinity and lower melting point and it is tougher and more processable than the polyketone copolymer [7]. By changing the sequence of carbon monoxide and alkene along the polymer chain, it is possible to control the UV-resistance of the polymer and it is even possible to make it photodegradable [5,8].

Polyketone is currently more than five times more expensive than polypropylene and it is therefore interesting to blend polyketone with the cheaper polymer. In this paper, the morphology, mechanical properties and oxygen barrier properties of polyketone/polypropylene blends are studied. In order to obtain good interfacial adhesion between the two components, a maleic-anhydride–polypropylene copolymer was added. At high temperature, the maleic-anhydride is hydrolysed and the resulting carboxylic groups are capable of forming hydrogen bonds with the polyketone [9] (Fig. 1a and b). In some of the blends, polyoxypropylenediamine was added to further improve the adhesion between the components. It has been shown earlier that covalent imide linkages are formed between maleic-anhydride–polypropylene copolymer and polyoxypropylenediamine chains and that this enhances their compatibility [9] (Fig. 1c). In the present blends, it is possible that covalent links are formed between the diamine and the polyketone chains as well as

* Corresponding author.
[1] Present address: Cederroth International AB, Box 715, SE-194 27 Upplands Väsby, Sweden.

0032-3861/01/$ - see front matter
PII: S0032-3861(00)00605-4

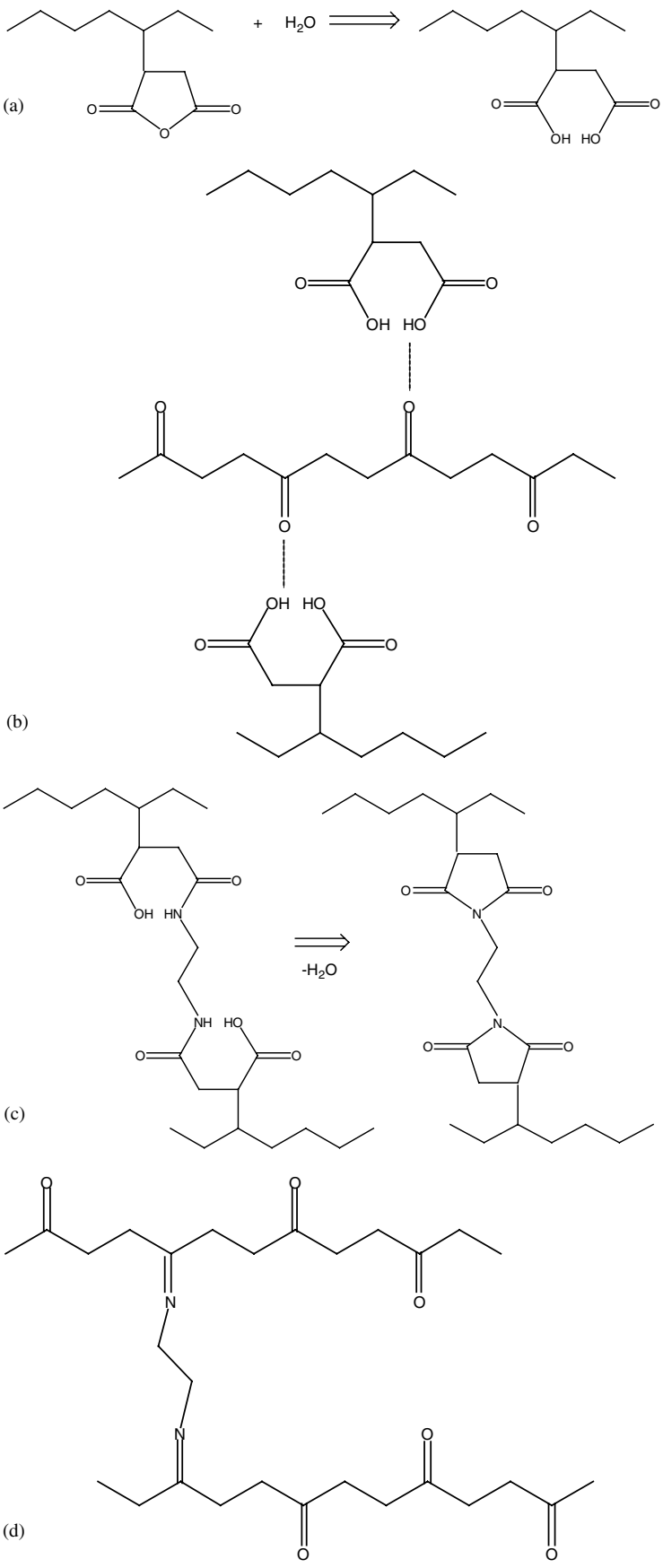

Fig. 1.

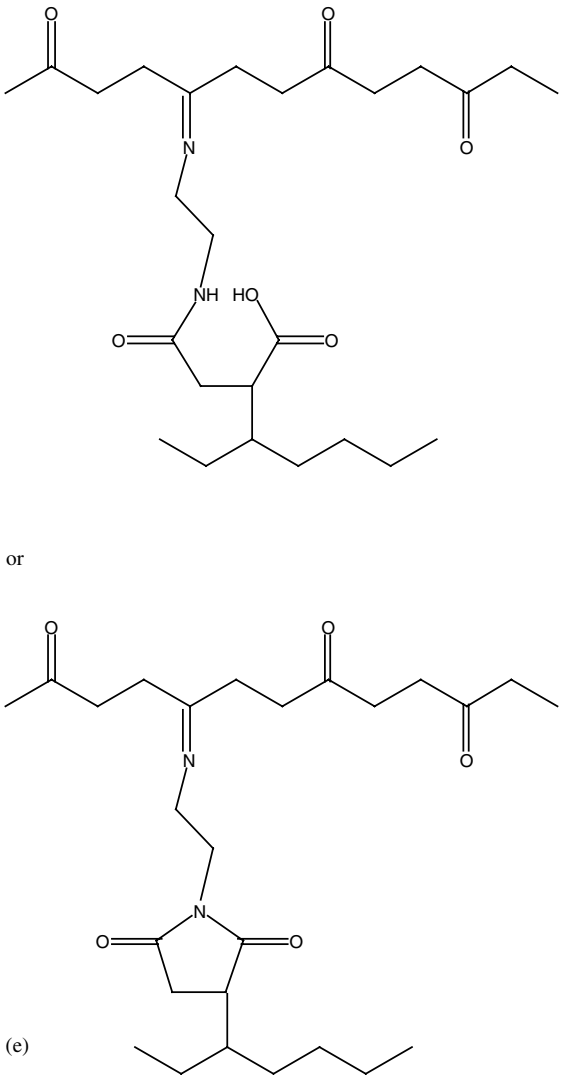

Fig. 1. (a) The hydrolysis at high temperature of maleated PP and the formation of carboxylic groups. (b) Hydrogen-bond formation between hydrolysed maleated PP and polyketone. (c) Covalent imine and imide links between the hydrolysed maleated PP and the diamine. Note that the chain length of the diamine is greater than is drawn in the figure. The imide link is formed at high temperature (>200°C [9]). (d) Covalent imine links between diamine and polyketone. Note that the chain length of the diamine is greater than is shown in the figure. (e) Covalent imine (upper) and imide (lower) links between hydrolysed maleated PP, diamine and polyketone. Note that the chain length of the diamine is greater than is drawn in the figure.

between the diamine, the polyketone and the polypropylene chains (Fig. 1d and e).

2. Experimental

2.1. Materials

The polypropylene (PP) used was a propylene–ethylene high impact copolymer (Amoco 300-CA06); $T_m = 167$°C, MFR (216°C/2.16 kg): 10 g (10 min)$^{-1}$ and elongation at break: 624%. The density was 910 kg m^{-3}. Two different polyketones were obtained from Shell Chemical Co. with molar masses: $\bar{M}_w = 175\,000$ g mol^{-1} (PKHM, Carilon D26HM100) and $\bar{M}_w = 100\,000$ g mol^{-1} (PKVM, Carilon D26VM100). PKHM had a melting point of 220°C, a density of 1240 kg m^{-3}, MFR (240°C/2.16 kg): 6 g (10 min)$^{-1}$ and an elongation at break greater than 300%. PKVM had a melting point of 220°C, a density of 1240 kg m^{-3}, MFR (240°C/2.16 kg): 60 g (10 min)$^{-1}$ and an elongation at break greater than 250%. The compatibilisers used were maleic-anhydride grafted polypropylene (maleated PP) homopolymers (Polybond 3150 and Polybond 3200) referred to as PB3150 and PB3200 and purchased from Uniroyal Chemical. PB3150 had a melting point of 157°C, a density of 910 kg m^{-3}, MFR (230°C/2.16 kg): 50 g (10 min)$^{-1}$, $\bar{M}_w = 330\,000$ g mol^{-1} and 0.5 wt% maleic-anhydride. PB3200 had a melting point of 157°C, a density of 910 kg m^{-3}, MFR (230°C/2.16 kg): 90–120 g (10 min)$^{-1}$, $\bar{M}_w = 120\,000$ g mol^{-1} and 1.0 wt% maleic-anhydride. Polyoxypropylene diamine (Jeffamine D-400 from Huntsman Corp.), referred to as diamine, was used in some blends as crosslinking agent. It had a density of 960 kg m^{-3} and a molar mass of 400 g mol^{-1}.

2.2. Sample preparation

2.2.1. Compounding/extrusion

The blends were made in a Berstorf ZE-25x33D twin-extruder. The pellets were mixed manually and dried prior to extrusion. The liquid diamine was blended with the solid components for 15 min in a large mixing container to ensure that diamine was properly adsorbed onto the individual pellets. The mixtures containing the diamine were rapidly decanted into the hopper to prevent accumulation of the diamine liquid at the bottom of the container. Screw and material feed speeds were optimised to obtain a continuous flow of polymer from the extruder. The strands from the extruder were cooled in water and pelletised using an Automatic ASG 51-strand pelletiser. The extrusion-temperature profile ranged from 245°C close to the hopper down to 209°C at the dye.

2.2.2. Compression moulding

Two grams of pellets were compression moulded between steel plates using Teflon sheets as anti-sticking agent in a Schwabenthan compression-moulding machine. The pellets were allowed to melt at 245°C for 4 min before a pressure of 3 MPa was applied for 3 min. Subsequently the samples were removed from the compression-moulding machine and allowed to cool in air.

2.2.3. Injection moulding

A Battenfeld, BM-C 800/2*300 Unilog 8000E was used to injection mould plates from predried extrusion-blended pellets. The melt temperature was 209–245°C and the mould temperature was 40°C. The injection speed was

50 rpm. A post-pressure of 3 MPa was applied for 10 s and the cooling time was 10 s.

2.3. Methods

2.3.1. Oxygen permeability measurements

The permeability of the materials to oxygen was obtained at 298.2 K using a Mocon OX-TRAN TWIN device. Samples with a thickness of 33–650 μm were mounted in an isolated diffusion cell and were subsequently surrounded by flowing nitrogen gas to remove absorbed oxygen from the samples. The sample had a circular exposure surface area of 5 cm^2 achieved by covering a part of the sample with a tight aluminium foil. One side of the specimen was initially exposed to flowing oxygen (1% hydrogen) at atmospheric pressure while the oxygen concentration was zero on the other side of the specimen. The flow rate (Q) through the specimen was measured during the transient period until the steady-state flow rate (Q_∞) was obtained. The diffusivity of oxygen D (assumed to be constant) was calculated by fitting the following equation to the $Q(Q_\infty)^{-1}$ versus t curve using a simplex search algorithm [10,11]:

$$\frac{Q}{Q_\infty} = \frac{4l}{(4\pi Dt)^{0.5}} \, e^{-l^2/4Dt} \tag{1}$$

where l is the thickness of the specimen. Assuming that Henry's law is valid, the solubility of oxygen (S) is given by

$$S = \frac{Q_\infty l}{Dp} \tag{2}$$

where p is the partial pressure of oxygen on the high oxygen pressure side of the specimen.

2.3.2. Scanning electron microscopy

Liquid-nitrogen-fractured and gold–palladium-sputtered specimens were analysed using a JEOL JSM-5400 and a JEOL JSM-840.

2.3.3. Shear viscosity

The shear viscosity was measured using a "plate-to-plate" Stress Tech Rheometer. The plate diameter was either 20 or 30 mm and the plate-to-plate gap was 0.2 mm. The rheometer was equipped with an "elevated temperature cell" coupled with an oven which ensured a constant temperature during the measurement. The sample cell was flushed with nitrogen to avoid thermal oxidation.

2.3.4. Density measurements

The density of the materials was obtained using the Archimedes principle, i.e. by comparing the weights of the sample in air and in ethanol with the densities of air and ethanol.

2.3.5. Infrared (IR) spectroscopy

A Perkin–Elmer 2000 FTIR-spectrophotometer, equipped with a Golden Gate accessory from Grasseby Specac, was used to obtain transmission and reflection IR spectra.

2.3.6. X-ray photoelectron spectroscopy (XPS)

The XPS spectra were recorded using a Kratos AXIS HS X-ray photoelectron spectrometer. The samples were analysed in a fixed analyser transmission (FAT) mode using a Mg Kα X-ray source operated at 240 W (12 kV/20 mA). The analysis area was approximately 1 mm^2. Detailed spectra for Si 2p, O 1s, N 1s and C 1s were acquired with a pass energy of 80 eV. The sensitivity factors used were 0.27 for Si 2p, 0.66 for O 1s, 0.42 for N 1s, and 0.25 for C 1s. These data were supplied by Kratos Analytical, Manchester.

2.3.7. Impact resistance

Specimens were tested in a Rosand Instrumental Falling Weight Tester. Approximately 10 specimens from each blend were tested. The striker with an impact load of 20 kg had a hemispherical head of radius 20 mm and the impact velocity was 3 m s^{-1}. The resistive force exerted by the specimen on the striker was monitored and the impact energy was calculated from the force–deflection curve up to the maximum load, i.e. the point of fracture.

2.3.8. Indentation tests

The indentation hardness was measured on specimens by a Buchholz-indentation durometer and a Zeiss SV11 light microscope. The metal block indentation tool was carefully placed on the specimen for 30 s and the resulting indentation length was measured from an enlarged photomicrograph. The Buchholz indentation hardness (BI) was calculated from the length of the indentation (ISO 2815-1973).

2.3.9. Differential scanning calorimetry (DSC) measurements

DSC thermograms on 5 mg samples were recorded between 60 and 240°C using a heating rate of 10°C min^{-1} in a Mettler TA8000.

3. Results and discussion

3.1. Compression-moulded specimens

The oxygen permeabilities of PKVM and PKHM are 12–20 cm^3 (STP) μm m^{-2} day^{-1} atm^{-1} which is only 1.4–3.3% of the permeability of polypropylene (902 cm^3 (STP) μm m^{-2} day^{-1} atm^{-1}). It would therefore be expected that blending polyketone into polypropylene would have a beneficial effect on the barrier properties of the latter. The oxygen permeabilities of the compression moulded PKVM-blends are shown in Fig. 2. The improvement of the barrier properties of the diamine-free blends was extensive; 23.9% by volume (30% by weight) of PKVM yielded a 70% decrease in oxygen permeability with respect to that of

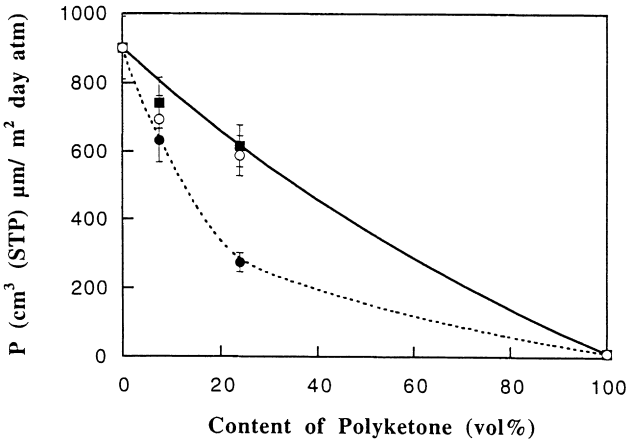

Fig. 2. Oxygen permeability as a function of the PKVM content. In addition to PKVM, the samples contain 5 wt% PB3200 (●), (○) and 5 wt% PB3150 (■). (○) and (■) also contained 1 wt% diamine. The rest was PP. The solid line is the prediction based on the Maxwell equation.

pure PP. The improvement of the barrier properties of the diamine-containing blends was modest and followed the predictions based on the Maxwell equation [12]:

$$P_o = P_{om}\left[1 + \frac{3(1 - v_m)}{\frac{q+2}{q-1} - (1 - v_m)}\right] \quad (3)$$

where q is the ratio of oxygen permeability of PKVM to that of PP and where P_o and P_{om} are the oxygen permeabilities of the blends and of the pure PP component, respectively. The Maxwell equation describes the impedance of a heterogeneous system of dispersed low-permeable spheres (PKVM) in a permeable matrix (PP, index m). v_m is the volume fraction of PP.

A similar plot for the PKHM-blends is given in Fig. 3. Both the diamine-free and the diamine-containing blends

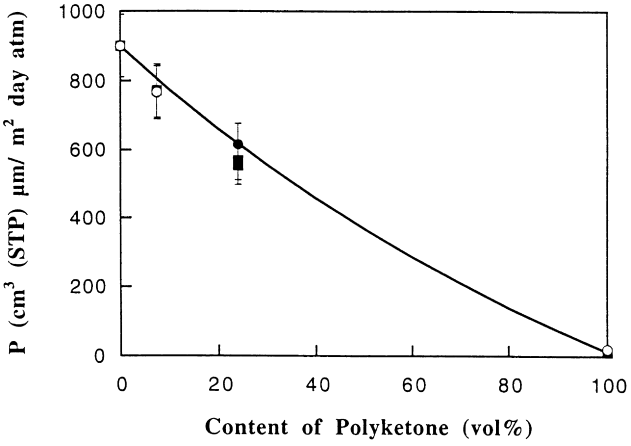

Fig. 3. Oxygen permeability as a function of the content of PKHM. Except PKHM the samples contain 5 wt% PB3200 (●), (○) and 5 wt% PB3150 (■). (○) and (■) also contain 1 wt% diamine. The rest is PP. The solid line is the prediction based on the Maxwell equation.

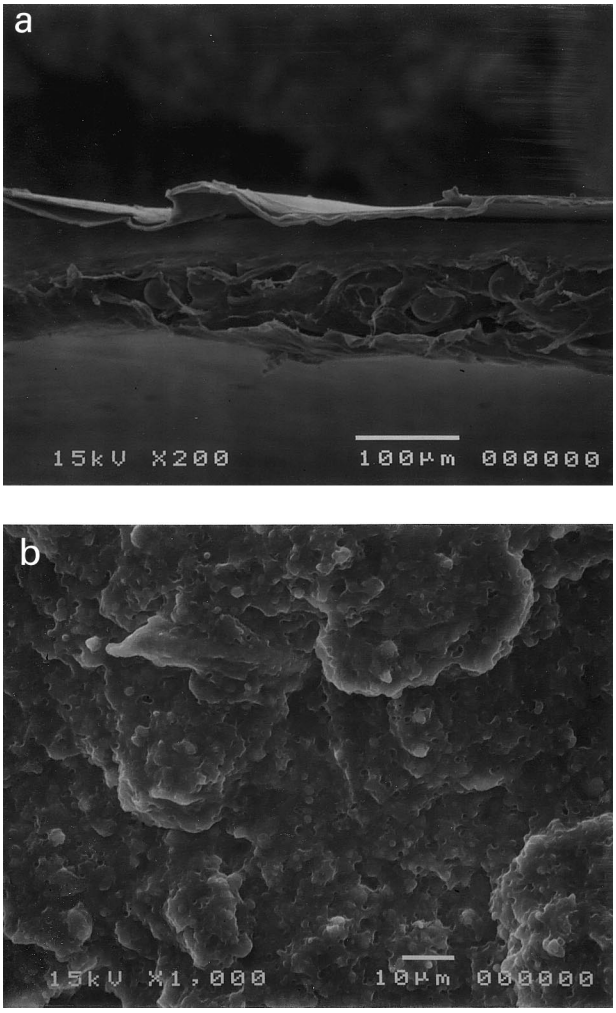

Fig. 4. (a) Scanning electron micrograph of a fracture surface of a specimen containing 65 wt% PP, 5 wt% PB3200 and 30 wt% PKVM (≈ 23.9 vol% PKVM). (b) Scanning electron micrograph of a fracture surface of a specimen containing 64 wt% PP, 5 wt% PB3150, 1 wt% diamine and 30 wt% PKVM (≈ 23.9 vol% PKVM).

followed the Maxwell equation. With the use of Eqs. (1) and (2), it was possible to divide the permeability into contributions from oxygen diffusivity and oxygen solubility. Although the scatter in these procedures is generally large, it seemed that the major beneficial effect was due to a decrease in oxygen solubility rather than to a decrease in oxygen diffusivity with increasing content of polyketone. The permeability data for the PKVM and PKHM blends may be explained on the basis of SEM information about the morphology. The morphology, in turn, is a consequence of the relative magnitudes in melt viscosity of the components.

Fig. 4a shows a typical morphology of the cross-section of a diamine-free PKVM blend. The compression-moulded diamine-free PKVM blends contain one or several clearly observable surface layers that seem to debond from the matrix upon freeze fracturing. It was possible to run IR spectroscopy on at least one of the surface layers and

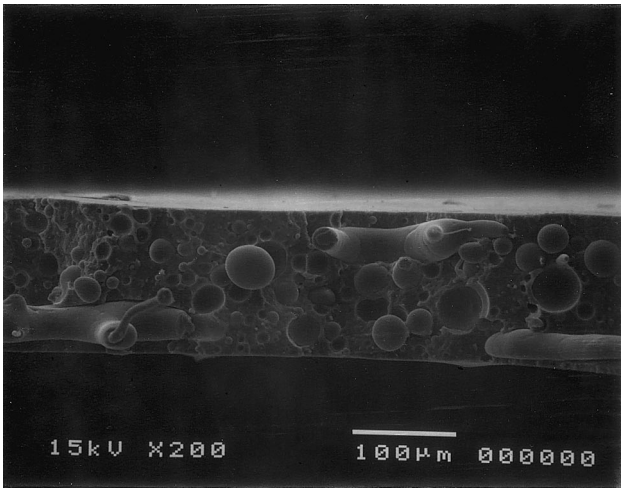

Fig. 5. Scanning electron micrograph of a fracture surface of a specimen containing 65 wt% PP, 5 wt% PB3200 and 30 wt% PKHM (≈ 23.9 vol% PKHM).

compare it with the interior of the moulded film. By comparing the relative intensities of the 810 cm^{-1} peak, which was observed in both PK and PP, and of the 840 cm^{-1} peak, which was observed only in PP, it was evident that the surface layer had a higher content of PKVM to PP than the core. The content of PKVM in the surface layer was estimated to be more than 80 wt% compared to the core which contained 30 wt% PKVM. Fig. 4b shows the morphology of a diamine-containing PKVM-blend. The surface looked brittle and smooth and there were basically no "pull-outs" of PKVM-particles which indicated that the bonding between the PKVM particles and the matrix was very good. The particles were smaller (diameters within a few microns) than in the diamine-free blends (compare Fig. 4a and b) which was also indicative of an enhanced compatibility between the polyketone- and the PP-rich components [13,14]. The absence of a PKVM-rich surface layer in these blends led to a less strong decrease in oxygen permeability (Fig. 2).

Fig. 5 shows the typical morphology of the diamine-free PKHM-blends. The absence of a large decrease in permeability with increasing polyketone content, such as that observed for PKVM, was due to the absence of a surface film. Even though PKHM-rich sheets were occasionally observed, most of the PKHM phase separated into relatively large spheres (10–50 μm). The diamine-containing PKHM blends showed the same morphology as the diamine-containing PKVM-blends. Density measurements revealed that the void content was small in all the blends. The maximum void content was 2% in the PKVM-blends and 3% in the PKHM-blends.

The difference in morphology between the diamine-free PKVM and diamine-free PKHM blends could be explained by viscosity data (Figs. 6 and 7). Fig. 6 shows that the low molar mass polyketone (PKVM) had a significantly lower melt viscosity than the high molar mass PKHM, which in

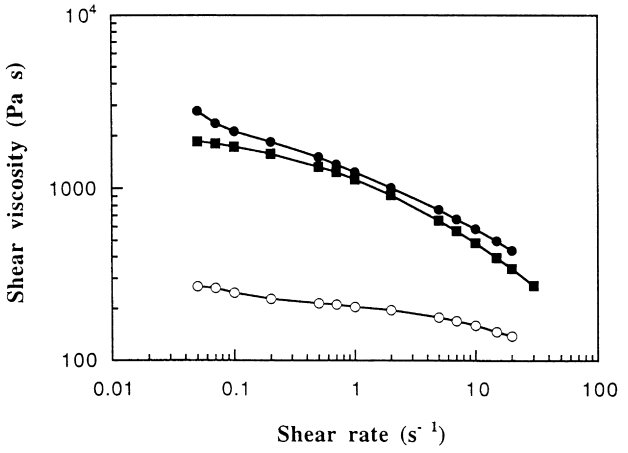

Fig. 6. Shear viscosity as a function of shear rate at 245°C for PKHM (●), PKVM (○) and PP (■).

turn possessed a viscosity higher than that of PP. The low viscosity of PKVM evidently allowed it to move to the surface region of the film during compression moulding, where it formed a continuous PKVM-rich PKVM/PP surface layer. A surface layer rich in the minor component was also observed when polyethersulphone (PES) containing a small amount of liquid crystalline polymer (LCP) was compression moulded [15]. The surface layer rich in LCP dramatically decreased the permeability to methanol of the blend compared to that of the pure PES. This morphology was completely absent in the high molar mass high viscosity PKHM-blends. Fig. 7 shows that the viscosity increased significantly with the introduction of diamine into the blends, which was considered to be indicative of the formation of strong covalent bonds between the diamine and the other constituents according to the suggested schemes in Fig. 1. As reported earlier for similar systems [9], the viscosity plateau-region at low shear rates vanished when diamine was added.

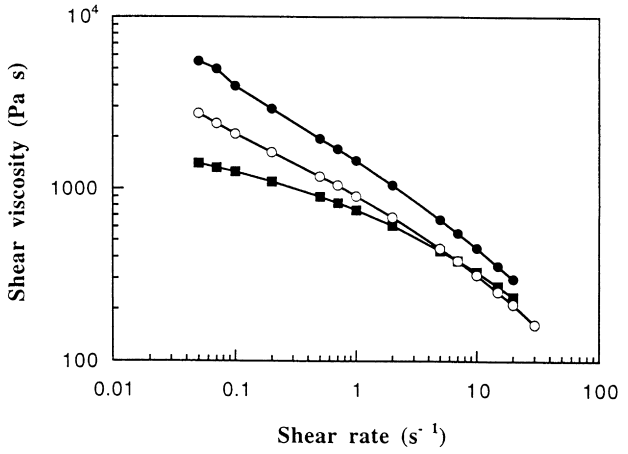

Fig. 7. Shear viscosity as a function of shear rate at 245°C for specimens containing 5 wt% PB3200, 30 wt% PKHM; and 65 wt% PP (●), 64.9 wt% PP and 0.1 wt% diamine (○) and 64 wt% PP and 1 wt% diamine (■).

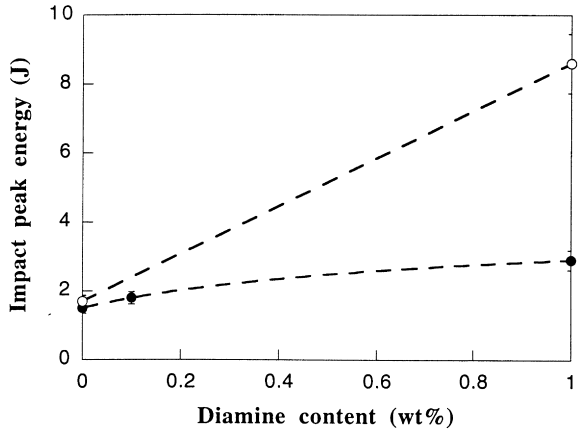

Fig. 8. Impact resistance at ambient temperature as a function of diamine content for injection-moulded plates containing 5 wt% PB3200, 30 wt% PKHM and 64–65 wt% PP (●) and 5 wt% PB3200, 10 wt% PKHM and 84–85 wt% PP (○).

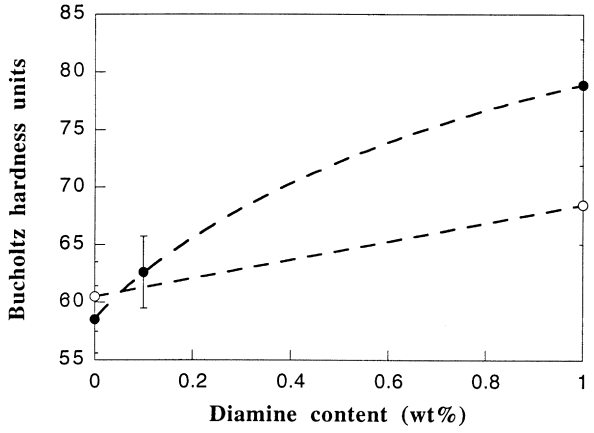

Fig. 9. Hardness at ambient temperature as a function of diamine content for injection-moulded plates containing 5 wt% PB3200, 30 wt% PKHM and 64–65 wt% PP (●) and 5 wt% PB3200, 10 wt% PKHM and 84–85 wt% PP (○).

IR spectroscopy indicated that maleic-anhydride in the PBs reacted with diamine to form imide links (Fig. 1c). This was observed by the lowering of the anhydride $(C{=}O)_2$ stretch at $\nu = 1750$ and 1850 cm^{-1} [9] and by the presence of a peak at 1703 cm^{-1} corresponding to imide. When diamine was added, the relative intensities of the peaks at 810 and 840 cm^{-1} decreased. This was suggested to be because polyketone formed imine links with the diamine (Fig. 1d and e). There were no traces of unreacted diamine in the blends, as indicated by the absence of absorption peaks at $\nu = 3450$–3280 and 1590–1600 cm^{-1} [9].

XPS, which samples the outermost 10 nm of the specimen, showed that the major constituent in this layer in the compression-moulded blends was PP, PP/PB3150 or PP/PB3200. A small peak at 288 eV for C 1s indicative of the presence of C=O appeared in the PKVM blends but not in the PKHM blends. Hence polyketone was present (<10 wt%) in the outermost layer in the PKVM blends but not in the PKHM blends.

3.2. Injection-moulded specimens

IR spectroscopy on injection-moulded specimens indicated, in accordance with data on compression-moulded specimens, that maleic-anhydride in the PBs reacted with diamine to form imide links and also that diamine formed imine links with polyketone. Also here traces of unreacted diamine were absent. By analysing the intensity of the polyketone C=O stretch through the thickness of the injection moulded plates it was concluded that polyketone was present throughout the cross-section.

SEM on injection-moulded diamine-free plates revealed elongated (thickness, 10 μm; length, 100 μm) polyketone-rich particles towards the surface and 10–20 μm sphere particles in the core, embedded in the PP matrix. The morphology was basically the same for both PKVM and PKHM blends and did not change with the polyketone content. The elongated particles were fewer in blends with 1% diamine. The size of the sphere-like particles in this blend was of the order of 1–10 μm. The fracture surface of these samples appeared brittle and "pull-outs" were absent, indicative of good bonding between the phases. The typical shell-core morphology of injection-moulded materials was hardly visible and it was also difficult to distinguish between the different components. The fracture-surface morphology of the diamine-containing samples was also here the same regardless of the molar mass of the polyketone and the content of polyketone.

The void content of the injection-moulded samples, as revealed by density measurements, was small. The void content was always lower than 5%, but it increased slightly with increasing concentration of polyketone. PKHM-blends had the highest void content. The addition of diamine resulted in a drop in void content by up to 4% (in void concentration) and for several diamine-containing specimens the void content was less than 1%.

The impact test showed that the impact strength of the pure polymers (PKHM, PKVM and PP) was substantially higher (20 29 J) than that of any of the blends. It therefore seems that the small amount of voids present in the blends was still sufficient to increase the brittleness. The addition of maleated PP led to a slight increase in toughness, but the most profound effect was observed after the addition of diamine, as shown in Fig. 8. Similar results were obtained when diamine was added to maleated PP/maleated rubber blends [9].

The hardness test showed that polyketone was much harder than polypropylene. In contrast to the impact testing, most of the blends here showed hardness values intermediate between those of the pure components. As in the case of toughness, the hardness increased with the addition of maleated PP and especially when the diamine was added (Fig. 9).

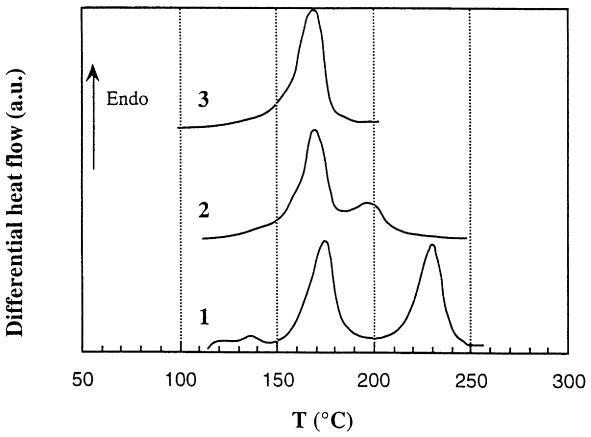

Fig. 10. Melting endotherms of an extruded blend containing 60 wt% PP and 40 wt% PKHM. The melting endotherms were recorded at a rate of 10°C min^{-1}. After each heating run the specimen was cooled at 20°C min^{-1}. The numbers indicate the number of the heating run.

3.3. Extruded specimens

The melting characteristics of the extruded samples were examined by repeated melting and crystallisation. All the PP/polyketone blends exhibited separate melting peaks after extrusion, indicative of separate crystallisation. Upon repeated melting and crystallisation of the two-component PP/polyketone blend, both the melting enthalpy and the melting peak temperature were lowered (Fig. 10, Table 1). It is known that polyketones may undergo polycondensation reactions in the melt, and the decrease in crystallinity and melting point observed here is probably due to the degradation of polyketone. It seemed that the degradation was catalysed by the presence of PP or of the maleated PP, since melting endotherms of the pure polyketones were basically unchanged upon repeated heating and cooling. The addition of diamine suppressed the crystallisation of polyketone after extrusion (Table 1). After a second thermal treatment, the crystallinity of polyketone was negligible and the crystallinity of PP decreased. This has been observed earlier [9]. There was probably a small amount of unreacted diamine left after extrusion that then reacted during the subsequent thermal treatment. It was thus expected that the compression-moulded and injection-moulded samples containing diamine would have a much lower degree of crystallinity than the other samples because these samples were exposed to a second thermal treatment in contrast to the extruded blends.

Table 1
Melting enthalpy of the polymers (J g^{-1})

Blends[a]	ΔH_m[b]	ΔH_m[c]	ΔH_m[d]	ΔH_m[e]
PP	88		96	
PKHM		84		86
PKVM		84		87
PB3200	87		93	
PB3150	94		95	
85/10/5[f]	78	60	83	33
84/10/5/1[f]	79	49	81	–
65/30/5[f]	79	63	86	52
64/30/5/1[f]	76	32	64	–

[a] The order is PP/PK/PB/diamine, mass per cent.
[b] Melting enthalpy for the PP or PP/PB component after extrusion.
[c] Melting enthalpy for the PK component after extrusion.
[d] Melting enthalpy for the PP or PP/PB component after extrusion and after a second thermal treatment which includes cooling at a rate of 20°C min^{-1}.
[e] Melting enthalpy for the PK component after extrusion and after a second thermal treatment which includes cooling at a rate of 20°C min^{-1}.
[f] Blends containing PB3200.

4. Conclusions

It has been shown that the oxygen barrier properties of PP may be significantly enhanced by blending the PP with a relatively small amount of polyketone. This was attributed to the formation of a polyketone-rich surface layer that occurred in blends with the low-viscosity polyketone. The low void content revealed that the phase adhesion between the different components was good. The addition of diamine yielded a network of covalent bonds between the maleated PP, the diamine and the polyketone. This lowered the crystallinity of the PP and of the polyketone. The presence of diamine enhanced the impact strength and the surface hardness.

Acknowledgements

A. Hellman and L. Höjvall, Packforsk are thanked for experimental assistance. B. Olander at the Department of Polymer Technology is thanked for experimental assistance with the XPS.

References

[1] Nobile MAD, Mensitieri G, Sommazzi A. Polymer 1995;36:4943.
[2] Sommazzi A, Garbassi F. Prog Polym Sci 1997;22:1547.
[3] Armer TA, Dangayach KC, Kastelic JR, Korcz WH, Dangayach K. Engng Plast Appl 1989;306:115.
[4] Chatani Y, Takizawa T, Murahashi S, Sakata Y, Nishimura Y. J Polym Sci 1961;55:811.
[5] Lommerts BJ, Klops EA, Aerts J. J Polym Sci: Polym Phys Ed 1993;31:1319.
[6] Starkweather HWJ. J Polym Sci: Polym Phys Ed 1977;15:247.
[7] Shell Carilon. Thermoplastic polymers information sheet.
[8] Leaversuch R. Mod Plast Int 1987;17:94.
[9] Phan TTM, Anthony J, DeNicola J, Schadler LS. J Appl Polym Sci 1998;68:1451.
[10] Pasternak RA, Schimscheimer JF, Heller J. J Polym Sci 1970;A2:467.
[11] Hedenqvist MS, Angelstok A, Edsberg L, Larsson PT, Gedde UW. Polymer 1996;37:2887.
[12] Hedenqvist M, Gedde UW. Prog Polym Sci 1996;21:299.
[13] Flodberg G, Hellman A, Hedenqvist M, Sadiku ER, Gedde UW. Polym Engng Sci 2000 (in press).
[14] Flodberg G, Höjvall L, Hedenqvist M, Sadiku ER, Gedde UW. Int J Polym Mater 2000 (in press).
[15] Wiberg G, Hedenqvist MS, Gedde UW. Polym Engng Sci 1998;38:1640.